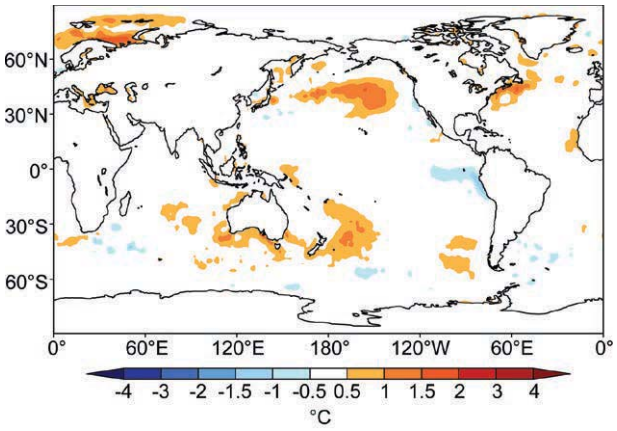

Fig. 4.33. Spatial distribution of average global sea surface temperature anomalies (°C, Reynolds et al. 2002) during 2013.

somewhat dissipated (see the partial reversal of the Atlantic Index, Fig. 4.35b), reducing the subsidence forcing on the Brazilian coast and hence helping explain the more favorable rainfall pattern in the second half of the year. The historical interplay of the SST gradient between the South and the North Atlantic is well depicted by the aforementioned Atlantic Index (Fig. 4.35b), which shows a predominance of negative conditions (unfavorable for convection within the South Atlantic ITCZ) over the last few years.

h. Atlantic warm pool—C. Wang

The Atlantic warm pool (AWP) is a large body of warm water in the lower latitudes of the North Atlantic Ocean, comprising the Gulf of Mexico, the Caribbean Sea, and the western tropical North Atlantic (Wang and Enfield 2001, 2003). Previous studies have shown that the AWP plays an important role in Atlantic TC activity, and provides a moisture source for North America, and thus affects rainfall

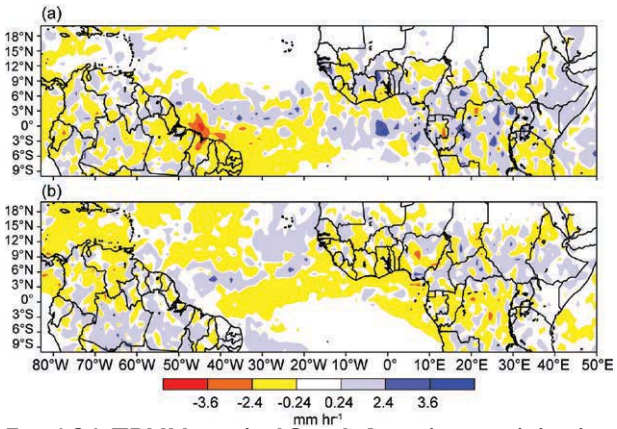

Fig. 4.34. TRMM tropical South America precipitation anomalies (mm hr^{-1}) with respect to 1998–2012 for (a) Jan–May 2013 and (b) Jun–Dec 2013.

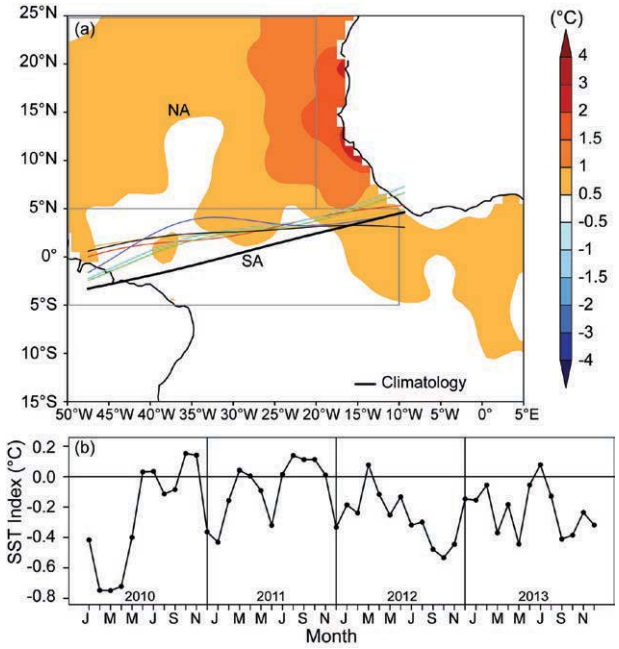

Fig. 4.35. (a) Atlantic ITCZ position inferred from outgoing longwave radiation during Mar 2013. The colored thin lines indicate the approximate position for the six pentads of Mar 2013. The black thick line indicates the Atlantic ITCZ climatological position. The SST anomalies (Reynolds et al. 2002) for Mar 2013 based on the 1982–2012 climatology are shaded. The two boxes indicate the areas used for the calculation of the Atlantic Index in 4.35b; (b) Monthly SST anomaly time series averaged over the South American sector (SA region, 5°S–5°N, 10°–50°W) minus the SST anomaly time series averaged over the North Atlantic sector (NA region, 5°–25°N, 20°–50°W) for the period 2010–13 forming the Atlantic Index. The positive phase of the index indicates favorable conditions for enhanced Atlantic ITCZ activity.

in the central United States (Wang et al. 2006, 2008a, 2011; Drumond et al. 2011). Unlike the Indo-Pacific warm pool, which straddles the equator, the AWP is normally north of the equator. Another unique feature of the AWP is that it does not exist in the boreal winter if the AWP is defined by SSTs warmer than 28.5°C (Wang and Enfield 2001). In addition to the large seasonal cycle, AWP variability occurs on both interannual and multidecadal timescales and has exhibited a long-term warming trend (Wang et al. 2006, 2008b). Figures 4.36a,b depict the long-term total and detrended June–November (JJASON) AWP area indices. The multidecadal and interannual variations of the AWP are displayed in Figs. 4.36c,d respectively.

The multidecadal variability (Fig. 4.36c) shows that the AWPs were larger during the period 1930–60, as well as after the late 1990s; and smaller during 1905–25 and 1965–95. The periods for large and small

SIDEBAR 4.1: THE 2013 ATLANTIC HURRICANE SEASON: BLIP OR FLIP?—C. T. FOGARTY AND P. KLOTZBACH

The 2013 Atlantic hurricane season threw a few "curve balls" for forecasters and was the "wild pitch" that triggered lengthy discussions among weather and climate scientists. What was predicted to be a very active season with at least seven hurricanes (about one-third of those projected to be major hurricanes) turned out to produce only two Category 1 hurricanes and just 20% of the predicted ACE. It was the quietest Atlantic hurricane season since 1994 in terms of major hurricanes (none), since 1983 in terms of ACE, and since 1968 for lowest peak intensity of the season's strongest storm.

Signals that convinced long-range forecasters to anticipate a very active season included anomalously-warm SSTs in the MDR, the absence of El Niño conditions, below-normal sea level pressures in the tropical Atlantic, and persistence of the positive phase of the AMO (Schlesinger and Ramankutty 1994) early in 2013, among other predictors. During neutral or negative phases of ENSO, upper-level wind shear in the tropical Atlantic is generally relatively weak. Neutral ENSO conditions were correctly predicted to be present by most forecast models during the 2013 hurricane season. The expectation that neutral ENSO conditions and a positive phase of the AMO would continue was key to the prediction of at least three major hurricanes—a relationship described by Klotzbach and Gray (2008).

The big question coming out of the season was "why so little activity when most standard pre-season predictors indicated favorable storm formation conditions?" The primary clue was found over the eastern tropical Atlantic and within the MDR where the peak of the season was characterized by enhanced subsidence. Additionally, SSTs evolved in an unusual manner with little warming in the MDR during the spring and first half of summer when surface water should be warming. While tropical Atlantic SSTs were warmer than normal, cool anomalies were evident in the subtropical eastern Atlantic during the early part of the hurricane season (Fig. SB4.1b). This area has been shown in several studies including Klotzbach (2011), to be a critical area for Atlantic hurricane activity. Cold anomalies in this region tend to generate stronger-than-normal baroclinicity, thereby contributing to cold upper-level lows, which enhance African easterly wave recurvature in the eastern part of the basin.

A similar pattern evolved in the higher latitudes of the North Atlantic. This evolution signalled what would be a short-term reversal of the longer-term positive phase of the AMO since the mid-1990s. These observations,

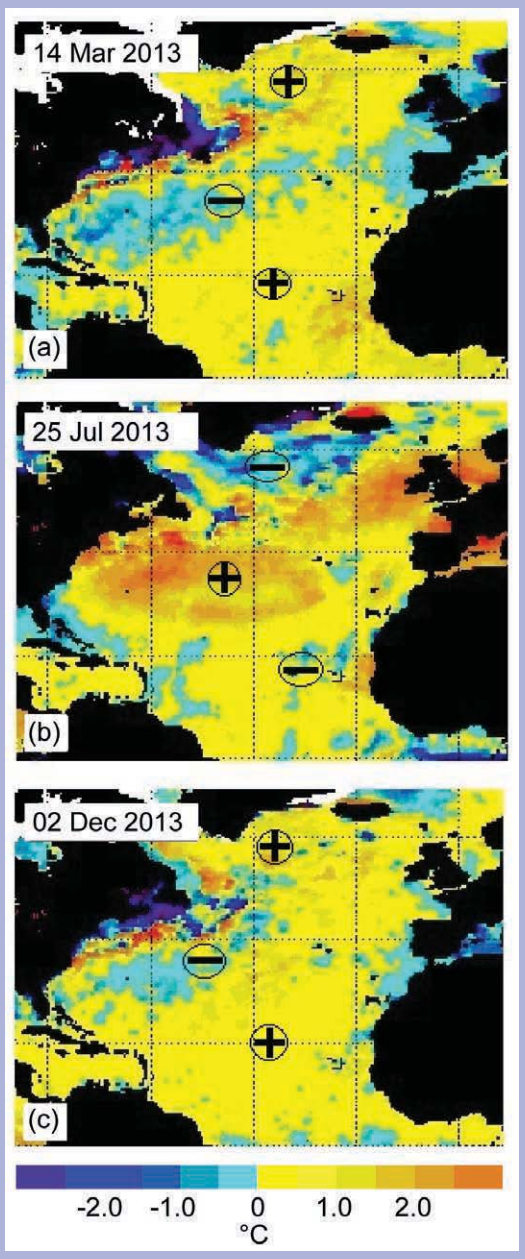

Fig. SB4.1. NOAA/NESDIS 50-km mean weekly SST anomaly (°C) for (a) 14 Mar, (b) 25 Jul, and (c) 02 Dec 2013.

however, raise more questions. Were the enhanced subsidence in the MDR and the "flat-lined" SST (see Fig. SB4.2) related? It certainly appears that way, given that the trade winds strengthened during that period which in turn arrested the usual warming of surface waters necessary to promote convective cloud formation. Dry air from the Saharan region was also advected into the MDR

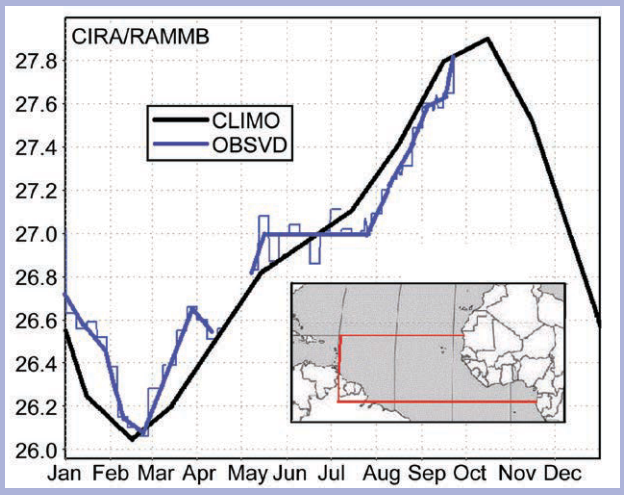

Fig. SB4.2. CIRA/RAMMB area-averaged SST throughout the MDR during 2013. Climatological values shown in black and observed shown in blue. Note the anomaly reversal from May to Jul.

by the enhanced trade winds. Another source of dry air (and wind shear) appeared to be from numerous cyclonic eddies diving southward during a commensurate reversal of the North Atlantic Oscillation (NAO) from negative to positive. Enhanced subsidence implies weaker easterly waves in the eastern Atlantic and a reduced likelihood of TC formation. Although convection was plentiful over the western part of the basin, above-normal vertical wind shear squelched the development of many storms that attempted to form there. Mid-tropospheric subsidence was also detected over the MDR (see http://typhoon.atmos.colostate.edu/).

From August to October the SST anomaly and AMO states returned to their early spring pattern almost as quickly as they deviated early in the year (the similarity between SST anomaly structures in Fig. SB4.1a and c is quite remarkable); however, it appears there was a lagged storm-suppressing impact that affected the MDR during the midst of the season. This intraseasonal change is a reminder that sometimes predictability may be limited to a shorter timeframe, and in the future sudden changes to the AMO cycle (or perhaps even the NAO) may serve as a shorter-term predictor within the season.

Two important questions remain: (1) Does potential exist to anticipate these sudden changes in the AMO? (2) Could the behavior in 2013 simply be a harbinger of a "flip" in the phase of the AMO from the current positive state to a negative one? The last time such a quiet season occurred was in 1994, at the end of the previous long-term negative phase of the AMO. There can be occasional "blips" in the phase or magnitude of the oscillation as seen in Fig. SB4.3. In 1968 there was a sharp drop in storm activity corresponding to a "dip" in the AMO index during that generally active era; however, the following year was extremely active. Data covering the past ~150 years of hurricane activity in the North Atlantic indicate that a period of ~60 years can be expected between peaks of hurricane activity, so the current active phase is more likely than not to persist for at least a few more years.

In summary, while many of the large-scale conditions typically associated with active TC seasons in the Atlantic were present (e.g., anomalously warm tropical Atlantic, absence of El Niño conditions, anomalously low tropical Atlantic sea level pressures), very dry midlevel air combined with midlevel subsidence and stable lapse rates to significantly suppress the 2013 Atlantic hurricane season. These unfavorable conditions were likely generated by a significant weakening of the strength of the AMO/Atlantic thermohaline circulation during the late spring and into the early summer. This very dry midlevel air is well-illustrated in figure 27 from last year's TC forecast verification report that shows the relative humidity anomalies at 600 hPa; that report is available at http://hurricane.atmos.colostate.edu/Forecasts/2013/nov2013/nov2013.pdf.

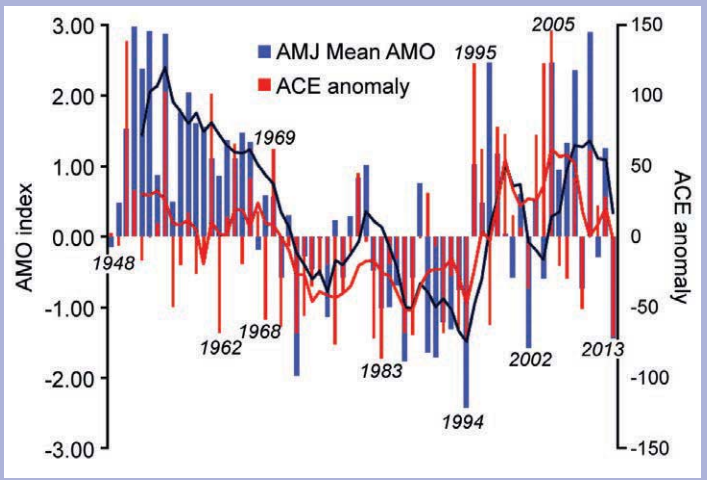

Fig. SB4.3. Apr–Jun (AMJ) mean of the AMO and season-total ACE anomaly from 1948 to 2013. Five-year running mean indicated with bold lines.

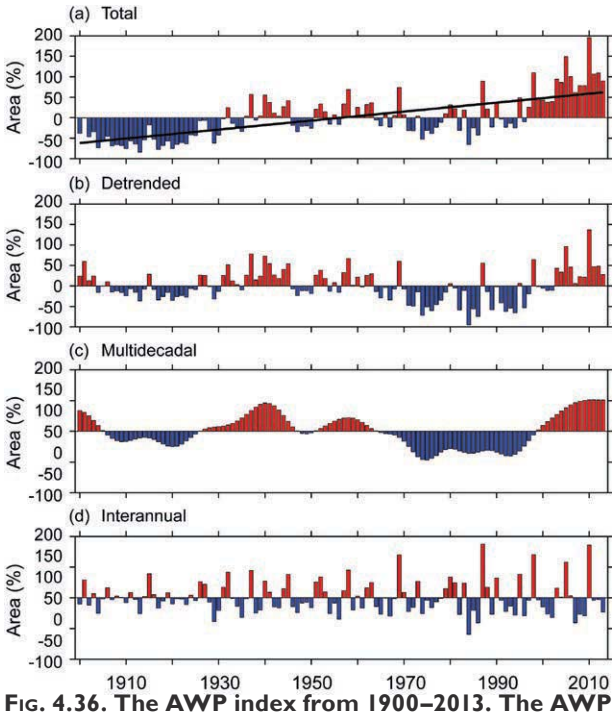

Fig. 4.36. The AWP index from 1900–2013. The AWP area index (%) is calculated as the anomalies of the area of SST warmer than 28.5°C divided by the climatological Jun–Nov AWP area. Shown are the (a) total, (b) detrended (removing the linear trend), (c) multidecadal, and (d) interannual area anomalies. The multidecadal variability is obtained by performing a seven-year running mean to the detrended AWP index. The interannual variability is calculated by subtracting the multidecadal variability from the detrended AWP index. The black straight line in (a) is the linear trend that is fitted to the total area anomaly. The extended reconstructed SST data set is used.

AWPs coincide with the warm and cool phases of the Atlantic multidecadal oscillation (AMO; Delworth and Mann 2000; Enfield et al. 2001). That is, AWP variability is tied to simultaneous alterations of SST in the high latitudes of the North Atlantic in a mode that operates primarily on a multidecadal timescale. Wang et al. (2008b) showed that the influences of the AMO on TC activity and climate might operate through the atmospheric changes induced by the AWP. The interannual AWP variability reflects both the local oceanic/atmospheric processes and the remote delayed influence of Pacific ENSO. The JJASON AWP interannual index of Fig. 4.36d is significantly correlated with the prior December–February (DJF) Niño3 region of SST anomalies, indicating a delayed ENSO effect on the AWP (Wang et al. 2008b). A recent study showed that the equatorial Amazon rainfall during the austral summer is negatively related to the following boreal summer's AWP SST, manifesting the remote ENSO impact on the AWP SST through its modulation of the Amazon rainfall (Misra and DiNapoli 2013). However, the contemporaneous correlation of the JJASON Niño3 SST anomalies and JJASON AWP index is not statistically significant. This reflects the facts that (1) large/small AWPs in the summer and fall have no clear relation to contemporaneous El Niño/La Niña development, and (2) by the summer and fall of the following year the Pacific El Niño/La Niña anomaly has almost always disappeared.

The AWP was larger than its climatological mean each month in 2013, with the largest AWP occurring in September (Fig. 4.37a). The AWP usually appears in May and peaks in September; however, the 2013 AWP variation was unique as it appeared early in March with a second peak in April. A new study demonstrates that the onset date of the AWP during 1979–2012 ranged from late April to early August (Misra et al. 2014). This indicated that the early onset of the 2013 AWP in March was the earliest onset during the recent decades. Because SSTs were warmer than 28.5°C in the equatorial western Atlantic from March 2013 (Fig. 4.37c), the AWP started to appear in March. In April, the warmer water in the equatorial western Atlantic further developed and merged with the warmer water in the equatorial eastern Atlantic (Fig. 4.37d). By May, the warmer water decayed in the equatorial western Atlantic (Fig. 4.37e). As in previous years, the AWP started to develop in June between the Gulf of Mexico and Caribbean Sea with the 28.5°C SST almost overlapped with the climatological AWP (Fig. 4.37f). By July and August, the AWP was well developed in the Gulf of Mexico and Caribbean Sea and reached eastward to the western tropical North Atlantic (Fig. 4.37g,h). By September, the AWP had further expanded southeastward and the isotherm of 28.5°C covered almost the entire tropical North Atlantic (Fig. 4.37i). The AWP started to decay after October when the waters in the Gulf of Mexico began cooling (Fig. 4.37j,k).

Previous studies have shown that AWP variability affects the Atlantic hurricane tracks (Wang et al. 2011). An eastward expansion of the AWP tends to shift the focus of cyclogenesis eastward, therefore decreasing the probability for hurricane landfall in the southeastern United States. A large AWP also weakens the North Atlantic subtropical high and produces the eastward TC steering flow anomalies along the eastern seaboard of the United States. Due to these two mechanisms, hurricanes are generally steered toward the north and northeast during a large AWP year. The TC steering flow anomalies in 2013

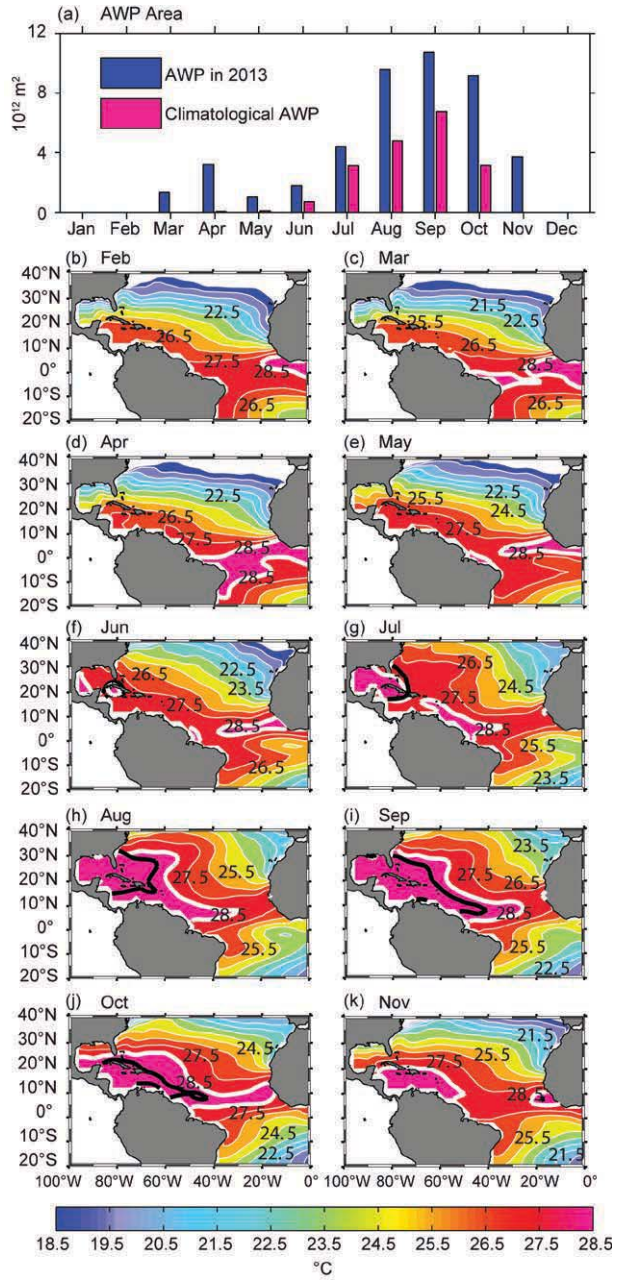

Fig. 4.37. (a) The monthly AWP area in 2013 (10^{12} m^2; blue) and the climatological AWP area (red) and the spatial distributions of the 2013 AWP in (b) Feb, (c) Mar, (d) Apr, (e) May, (f) Jun, (g) Jul, (h) Aug, (i) Sep, (j) Oct, and (k) Nov. The AWP is defined by SST larger than 28.5°C. The black thick contours in (f)–(k) are the climatological AWP based on the data from 1971–2000 and the white thick contours are the 2013 28.5°C SST. The extended reconstructed SST data set is used.

were consistent with those of the observed large AWP years (Wang et al. 2011).

During the 2013 Atlantic TC season, the TC steering flow anomalies were characterized by an anomalous cyclone and an anomalous anticyclone (Fig. 4.38). Associated with these patterns were mostly the eastward and southeastward flow anomalies in the western tropical North Atlantic, and the northward and northeastward flow anomalies in the open ocean of the North Atlantic. An exception was in November during which the TC steering flow anomalies were westward in the hurricane MDR (Fig. 4.38f), but only one storm, Melissa, formed southeast of Bermuda during that month. The distribution of the 2013 TC steering flow was unfavorable for TCs to make landfall in the southeastern United States. While a large AWP is consistent with the fact that no storms made landfall in the southeastern United Stated in 2013 (either by decaying or moving northward or northeastward), the AWP had no apparent enhancing effect on the number of TCs for the North Atlantic TC season (section 4d2) as a large AWP typically results in more TCs (Wang et al. 2006).

i. Indian Ocean dipole—J.-J. Luo

Interannual climate variability in the tropical Indian Ocean (IO) is driven either by local ocean-atmosphere interactions or by the Pacific ENSO in the presence of interbasin interactions (e.g., Luo et al. 2010). The Indian Ocean dipole (IOD) is one major internal climate mode in the IO that may induce considerable climate anomalies in many countries surrounding the IO. The IOD normally starts in boreal summer, peaks in Northern Hemisphere fall, and declines rapidly in early boreal winter. During May–September 2013, a negative IOD (nIOD) event occurred, characterized by anomalous SST warming in the tropical eastern IO and cooling in the west. Compared to previous events in 1990, 1992, 1996, 1998, 2001, 2005, and 2010 (Luo 2011), the 2013 nIOD was short-lived and weak with warming anomalies in the eastern IO of <0.5°C and a maximum cooling anomaly in the west of about −0.4°C in July (Fig. 4.39). The east warming/west cooling SST dipole structure is linked with stronger-than-normal surface westerlies in the central equatorial IO (Ucio) as noted in Fig. 4.39b; and this is reminiscent of the canonical air-sea coupled feature of nIOD. Note that this nIOD signal occurred along with a weak cooling condition in the Pacific. Such co-occurrence of IOD and ENSO has been found often in the historical records.

SSTs in major parts of the tropical IO during 2013 were warmer than normal except the western IO during June–August (Fig. 4.40). This may be partly due to the rapid rise of the IO SST over past decades in response to increasing greenhouse gas emissions (Hoerling et al. 2004). The fast surface warming in